Confinement degradation of ELMy H modes at high density and/or radiated power fraction

1999 Nucl. Fusion 39 1687

(http://iopscience.iop.org/0029-5515/39/11Y/308)

Confinement degradation of ELMy H modes at high density and/or radiated power fraction

JET Team* (prepared by G.F. Matthews)
JET Joint Undertaking,
Abingdon, Oxfordshire,
United Kingdom

Abstract. High density, high radiated power fraction and small ELMs are key elements of the current ITER design. In JET, these conditions are shown to be associated with high ELM frequency, low pedestal pressure and correspondingly reduced global energy confinement time. The article reviews the current understanding of the connections between these parameters and the mechanisms for the saturation of the density with gas fuelling.

1. Introduction

The existing ITER design requires a density at or above the Greenwald density limit ($f_{GL} = \bar{n}_e/\bar{n}_{e,Greenwald} > 1.1$) [1], combined with a high energy confinement time (for ignition $f_{GL}H_{97} > 1.1$ using the ITERH-97P(y) scaling [2]). High total radiated power fraction is also required to protect the divertor [3] (excluding bremsstrahlung, $f_{rad} \geq 0.75$). There are three critical issues which have not received much attention in energy confinement scaling studies: (a) degradation of τ_E with f_{GL} [4, 5]; (b) degradation of τ_E with f_{rad}; and (c) failure of f_{GL} to increase with gas fuelling rate [4–6]. This article reviews recent JET results which have advanced our understanding in these areas.

Figure 1(a) shows the variation of the normalized Lawson product $f_{GL}H_{97}$ as a function of the Greenwald density fraction f_{GL} for low triangularity H modes ($\delta < 0.24$). These pulses were unfuelled, had strong deuterium fuelling or had seeding with neon or nitrogen impurity (points selected with total radiated power fraction $f_{rad} > 0.4$, excluding neutral losses). Deuterium gas fuelling results in a modest increase in density but the normalized Lawson product is not increased. At higher fuelling rates the discharges return to L mode and disrupt in exactly the same way as L mode discharges [8]. The upper limit in density and confinement is very similar for impurity seeded and deuterium fuelled discharges. As deuterium fuelling rate is increased, the type I ELM frequency rises until at some point the frequency jumps up owing to the onset of higher frequency type III ELMs. It is at this point that the greatest loss in energy confinement is observed [4, 5]. With impurity seeded discharges, without significant deuterium fuelling, the type I ELM frequency decreases until there is a sudden jump to high frequency type III ELMs, at which point ∼25% of the stored energy is lost [9]. In both cases intermediate states can also be produced where there are compound ELMs which appear to be a mixture of type I and type III ELMs.

Figure 1(b) shows data from deuterium fuelling scans into 2.5 MA/2.5 T H modes in the MkIIa divertor in which the plasma triangularity was varied [7]. The data show that increasing the plasma triangularity raises the main plasma density at which the confinement degrades. High triangularity pulses have a lower ELM frequency for a given gas fuelling rate and plasma density.

2. Degradation of H mode pedestal

2.1. Relationship between ELM frequency and confinement

The roll-over in energy confinement at high density and/or radiation appears to be dominated by changes in time averaged pedestal pressure with ELM frequency, f_{ELM} [10]. Figure 2(a) shows this relationship for D_2 and N_2 seeded discharges at fixed current and input power.

The pedestal pressure cycles seen in JET during ELMs have an asymptotic form which for given field and current are almost independent of ELM frequency, as in the example of Fig. 2(b). The equation describing this time evolution is [10]:

$$P_{ped}(t) = P_{min} + (P_{max} - P_{min})(1 - e^{-t/r}) \qquad (1)$$

where P_{min} is the pressure to which the pedestal crashes after an ELM, P_{max} is the saturation

* See Nucl. Fusion **39** (1999) 1227.

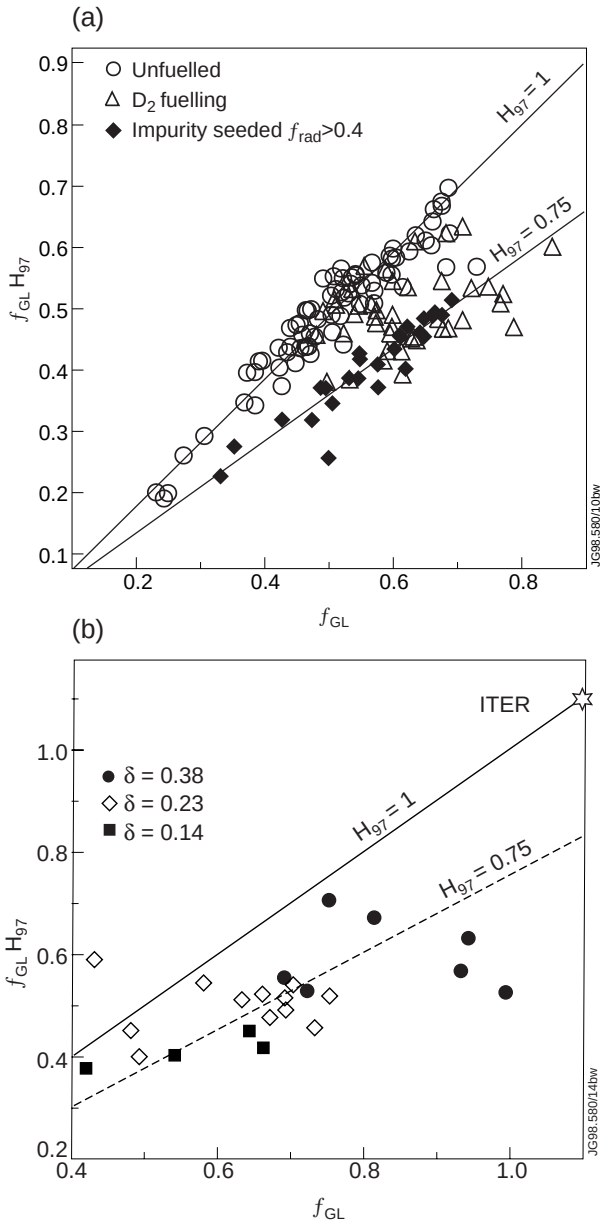

Figure 1. $f_{GL}H_{97}$ versus f_{GL} (a) for unfuelled, impurity seeded and D_2 fuelled H modes in the JET MkI and MkIIa divertors for I_p = 1.9–2.9 MA and triangularity $\delta < 0.24$, and (b) for a triangularity scan in MkIIa with D_2 fuelling for identical I_p and P_{NBI} [7].

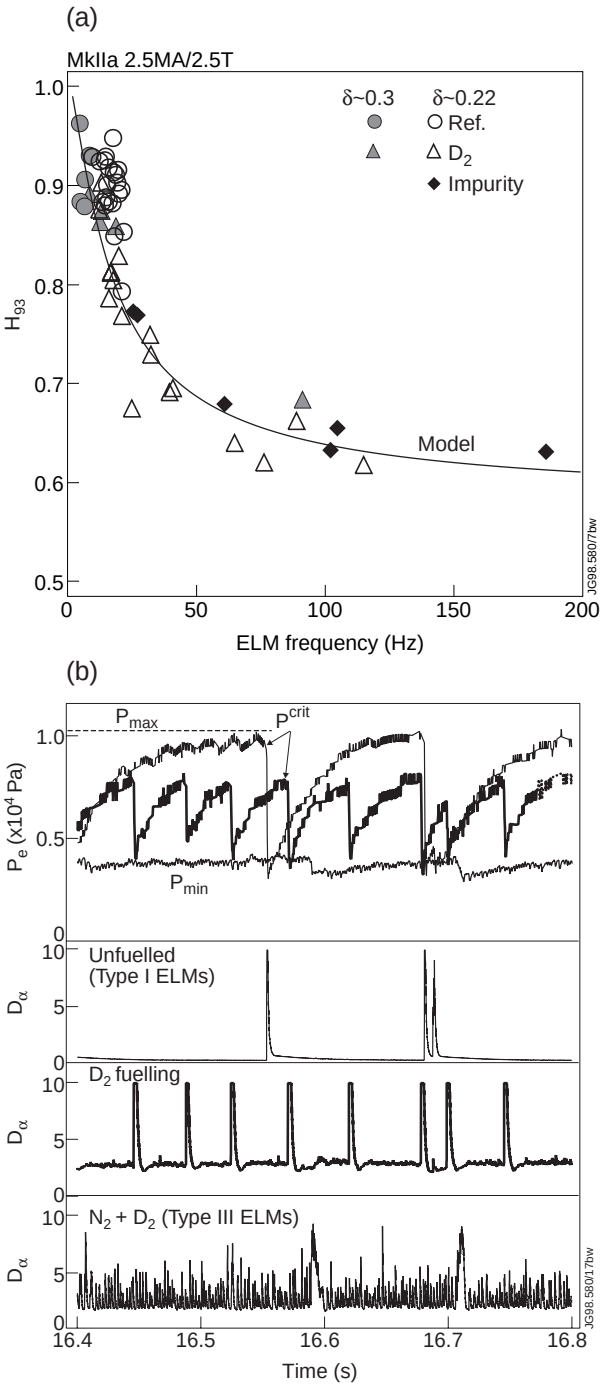

Figure 2. (a) H_{93} versus ELM frequency from experiment and model, and (b) pedestal P_e cycles and divertor D_α versus time for an unfuelled discharge and identical pulses with D_2 and D_2 + N_2 fuelling [10].

pressure which would pertain in the absence of an ELM and τ is the edge reheat time. From a time average of (1) an equivalent expression for confinement time can be derived [10]:

$$H_{93} = f_{93}^{prof} - f_{93}^{ped}\left[f\tau(1 - e^{-1/f\tau})\right] \qquad (2)$$

where f is the ELM frequency, f_{93}^{prof} is the upper limit in H factor at zero ELM frequency and f_{93}^{ped} is the maximum amount by which the H factor is degraded at high ELM frequency. It is more consistent to apply this model to the ELM free ITERH-93P scaling since ITERH-97P(y) is already a fit to

an ELMy data set. Figure 2(a) compares Eq. (2), using $\tau = 0.034$, $f_{93}^{prof} = 1.02$ and $f_{93}^{ped} = 0.44$, with data from the JET MkIIa campaign ($I_p = 2.5$ MA, $B_T = 2.5$ T and $P_{NBI} = 12$ MW). Both low and high triangularity pulses fit the model well. The main effect of increasing the triangularity is to lower the ELM frequency at a given density. The same model fits a wider range of plasma current (1.8–4.8 MA) and neutral beam power with the additional assumption that $\tau/\tau_E = 14$ [10].

2.2. Pedestal width scalings and the type I to type III ELM transition

The relationships discussed in the previous sections show how confinement varies with ELM frequency, but what controls ELM frequency? Good confinement is generally associated with type I ELMs, which are thought to occur when the edge pressure gradient reaches the ideal ballooning limit. If this is true then the critical pressure gradient for type I ELMs is expected to scale as [11]:

$$P^{crit}/\Delta \propto I_p^2 S^y \tag{3}$$

where I_p is the plasma current, S is the edge magnetic shear and Δ is the pedestal width. The edge pressure evolves with time according to Eq. (1) until it reaches P^{crit}. Figure 3 shows fits to the P^{crit} data for type I ELMs in unfuelled discharges for a range of S (2.9–4), I_p (1.7–2.9 MA), B_T (1.7–2.9 T) and isotopic mass (H, D, T), with Δ assumed to be proportional to either the fast ion Larmor radius, $P^{crit} \propto I_p^2 S^2 \rho_{i,fast}$, or the thermal ion Larmor radius, $P^{crit} \propto I_p^2 S^2 \rho_{i,thermal}$.

Although in this data set the fit which assumes that the width is proportional to $\rho_{i,fast}$ is slightly better than that for $\rho_{i,thermal}$, the uncertainties are such that one cannot use this method to distinguish between the two models. A similar analysis of gas fuelling scans shows a better fit to the scaling with $\rho_{i,thermal}$ than $\rho_{i,fast}$ [12]. This difference might be attributed to the effect of gas fuelling on the fast particle population but the issue is as yet unresolved. The attraction of the fast particle picture is that it allows a qualitative explanation of other phenomena. For example:

— In hot ion H mode, tritium NBI into a deuterium plasma produces a similar pedestal pressure to that for tritium injection into a tritium plasma, which is higher than that for deuterium injection into deuterium [13, 14].

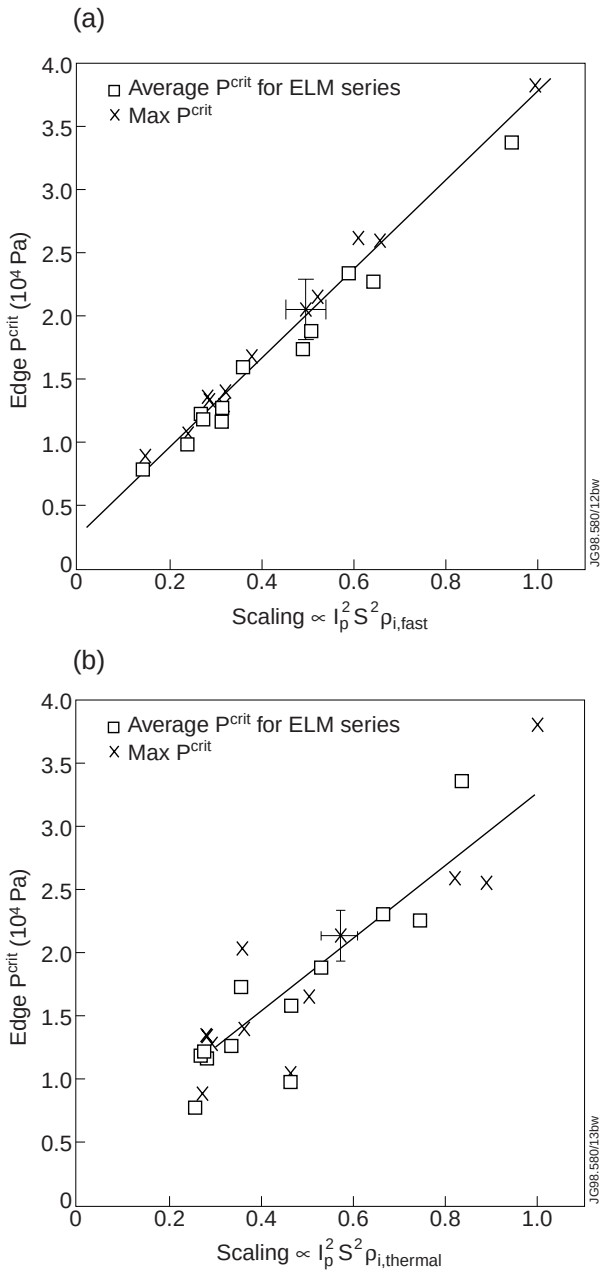

Figure 3. P^{crit} versus normalized scaling expression for (a) fast ions and (b) thermal ions [11].

— In hot ion H mode, P^{crit} for the first ELM is higher for 140 keV NBI than it is for 80 keV at identical edge ion temperature.

— On-axis ICRH, which produces relatively low edge fast particle populations, is characterized by high frequency type III ELMs and correspondingly low edge pressure when compared with neutral beam heated discharges at the same input power (Fig. 4).

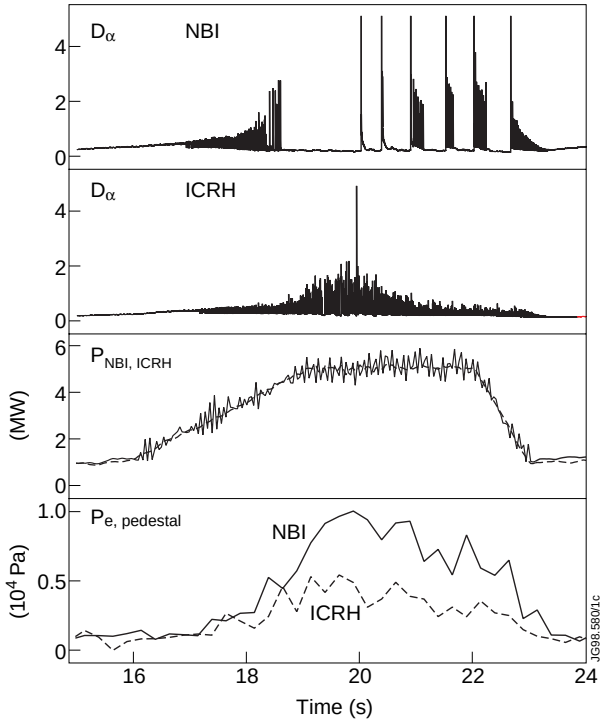

Figure 4. Comparison of edge pressure and D_α for radiofrequency and neutral beam generated ELMs.

Whether the pedestal width scales as the fast or thermal ion poloidal Larmor radius, the loss in confinement and rise in type I ELM frequency with gas fuelling can be associated with a cooling of the edge. In the limit of low or high T_e, the energy of fast particles is expected to be constant. In JET, however, the edge plasma is in a transitional regime and the mean fast ion energy derived from Fokker–Planck calculations varies between 30 and 50 keV.

A critical question for understanding the loss of energy confinement at high density and/or radiation is what causes the transition to type III ELMs. There are two possibilities currently under consideration:

— Collisionality may be the critical parameter for transition to type III ELMs, possibly owing to the onset of resistive ballooning instabilities [15].
— Non-ambipolar losses of fast particles within one poloidal Larmor radius of the separatrix may create a radial electric field and hence the velocity shear which stabilizes the pedestal region. For this to happen, a critical density of fast particles at the edge of the pedestal would be required. Strong gas fuelling may deplete the fast particle population through charge exchange processes, thus leading to a transition from type I to type III ELMs [14].

The hypothesis that depletion of the edge fast ion population is responsible for the type I to type III ELM transition is difficult to prove. Analysis of trace tritium transport experiments has highlighted the fact that current models do not correctly predict the fast particle population near the edge of the plasma [16]. The observed anomaly is also found to be dependent on gas puffing. Existing Fokker–Planck calculations of the neutral beam deposition do not contain an adequate description of the edge charge exchange losses. However, they do show the lowest fast ion energies and densities in the strongly fuelled and impurity seeded plasmas. Thus, although the trends are qualitatively correct, a causal relationship between fast ion density and the transition from type I to type III ELMs cannot be demonstrated quantitatively.

Deuterium fuelling of type I ELMy H modes clearly raises the collisionality at the pedestal. However, impurity seeding, combined with low deuterium fuelling rates, can produce type III ELMs at much lower line averaged density (Fig. 1(a)). It therefore appears possible to produce type III ELMs at a pedestal collisionality ($\propto nZ_{eff}/T_e^2$) that is up to an order of magnitude lower than is observed in equivalent type I ELMy discharges. Another argument against collisionality as the sole cause of the type I to type III ELM transition is that type III ELMs are observed in ICRH heated discharges despite lower collisionality. In the example of Fig. 4, the collisionality at the top of the pedestal is ten times lower in the ICRH heated discharge than in the NBI case. If it is the collisionality at the separatrix which is important [15], then the situation is not so clear-cut. Our analysis indicates that the collisionality near the separatrix can be very similar with type I and type III ELMs, but the analysis is inconclusive.

Despite the loss in pedestal pressure associated with ICRH heated H modes, the global energy confinement time, after corrections for the fast ion contributions to the energy, is as good as in the best type I ELMy H modes with neutral beam heating. Local transport analysis with the TRANSP code shows that the core χ_{eff} profiles in such cases are identical. The reason for the similarity in the global energy confinement time is that the power deposition profile for ICRH heated discharges is strongly peaked on-axis while for neutral beam heated ELMy H modes it is almost flat [11]. Owing to the lack of strong profile resilience seen in JET, this difference results in a peaking of the core pressure profiles of ICRH heated discharges which almost exactly

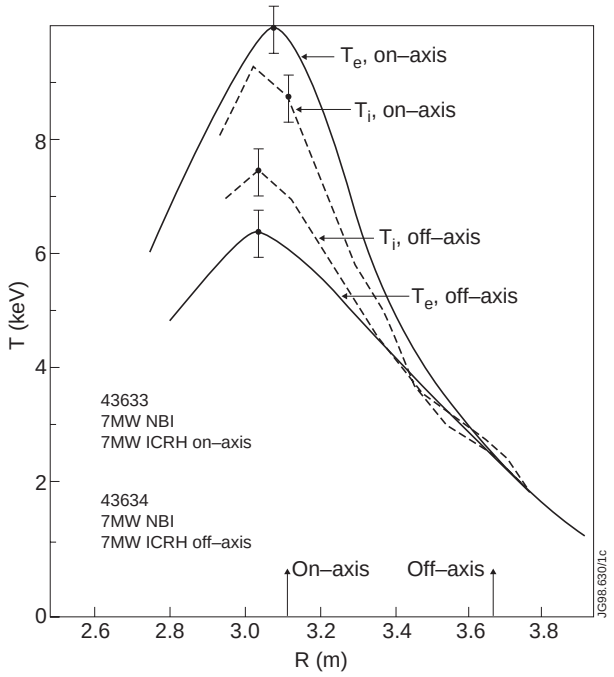

Figure 5. Comparison of two pulses with combined heating at identical density and Z_{eff}. In one case, the ICRH is on-axis; in the other, it is at $r/a = 0.75$, resulting in a flattening of the ion and electron temperature profiles inside the heating radius.

cancels the loss in pedestal pressure. In Fig. 5, the absence of strong electron or ion temperature profile resilience is demonstrated with a pair of discharges in which combined heating was applied. In one case, on-axis ICRH was used and in the other it was moved out to a radius of $r/a = 0.75$. Both discharges had a line averaged density of 3.5×10^{19} m^{-3} and identical Z_{eff}. The absence of a specific description of the pedestal scaling is thus not the only deficiency of existing global energy confinement scalings. The power deposition profile predicted for alpha particle heating in ITER has a shape which lies about halfway between the NBI heating and ICRH profiles in JET. This would be expected to offset partly any loss in pedestal energy associated with the need to operate with small high frequency ELMs.

3. Effect of radiation and gas fuelling on core transport

Experiments at JET have been aimed at establishing whether the core confinement of strongly radiating pulses is consistent with gyro-Bohm

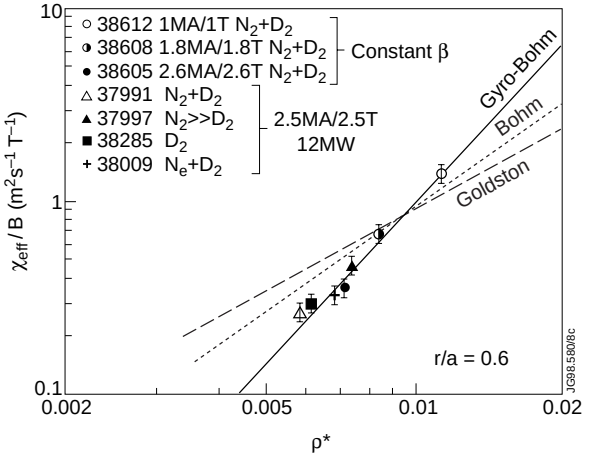

Figure 6. Logarithmic plot of χ_{eff}/B (TRANSP) versus ρ^* at $r/a = 0.6$ for a variety of impurity and deuterium seeded discharges. Pulses 38612, 38608 and 38605 form a ρ^* scan at constant β (but ν^* varies).

scaling, as is the case for type I ELMy discharges [17]. Previous global confinement analysis pointed to Bohm-like behaviour which would be very unfavourable for ITER [18]. Recent local transport analysis of dimensionless scaling experiments in the radiative regime [19] has confirmed that, provided that the effect of variations in collisionality is negligible, the scaling of χ_{eff} in the core is most consistent with gyro-Bohm scaling (Fig. 6). Gas fuelled pulses also seem to fit the same line. Near the edge of the plasma ($r/a > 0.75$) the transport scaling becomes more Bohm-like ($\chi_{eff}/B \propto \rho^{*1.6}$). How the width of this region scales is not clear at present. When JET is run in a similar range of dimensionless parameters to the ASDEX Upgrade completely detached H mode [20], the H_{93} factors are very similar. As JET moves to its normal range of dimensionless parameters (ρ^* and ν^*) the performance with respect to the H_{93} scaling decreases [19], which is a consequence of the less favourable scaling of the plasma edge.

4. Density saturation in H mode

Three distinct explanations have been advanced for H mode density saturation:

(a) At high fuelling rates, fuelled particles find it increasingly difficult to penetrate the H mode transport barrier, either as ions or neutrals, and so the density saturates.

(b) Particle transport degrades in proportion to the rise in ionization sources. The saturation is then caused by higher losses at higher fuelling rates.
(c) Separatrix density saturates with fuelling rate as a result of detachment in the scrape-off layer (SOL) [21]. If there is also a fairly rigid relationship between separatrix and pedestal density, then saturation of the separatrix density implies clamping of the core density.

Recent JET experiments have helped to distinguish between these three broad classes of mechanism.

4.1. Trace tritium experiments

Short puffs of tritium were used as test particles during a deuterium fuelling scan. Tritons are ideal test particles since they are very similar to the principal plasma species, yet their progress through the plasma can be monitored using neutron detectors [16]. Figure 7 illustrates the ELM characteristics and density behaviour of a series of H mode discharges with increasing deuterium fuelling into which a short tritium puff was introduced. From the DT neutron yield the increment in the total triton content can be calculated and compared with the increment in total electron content. This comparison is made in Fig. 8 for selected H modes from Fig. 7 and an L mode case. In L mode the total electron content jumps up, as expected, at the time of the tritium puff. In H mode, however, no corresponding step in electron content is observed. The peak triton content corresponds to $(20 \pm 5)\%$ of the tritium gas puff in all cases.

In H mode, therefore, the plasma behaves like a bucket filled to the brim. The tritons which are added penetrate the plasma with relative ease but other plasma particles are displaced to accommodate them. It is possible that it is ELMs which expel the excess particles, but in these experiments this issue could not be resolved. Changes in the time averaged core particle transport shown in Fig. 9, as determined from the time evolution of the neutron profile [16], are too small to explain the density saturation [6].

These results demonstrate that it is not simply failure of gas fuelled ions to penetrate the core plasma which results in density saturation or changes in core particle transport. The key to understanding the density saturation therefore lies in understanding the region between the top of the pedestal and the separatrix, which are inaccessible to the trace tritium analysis.

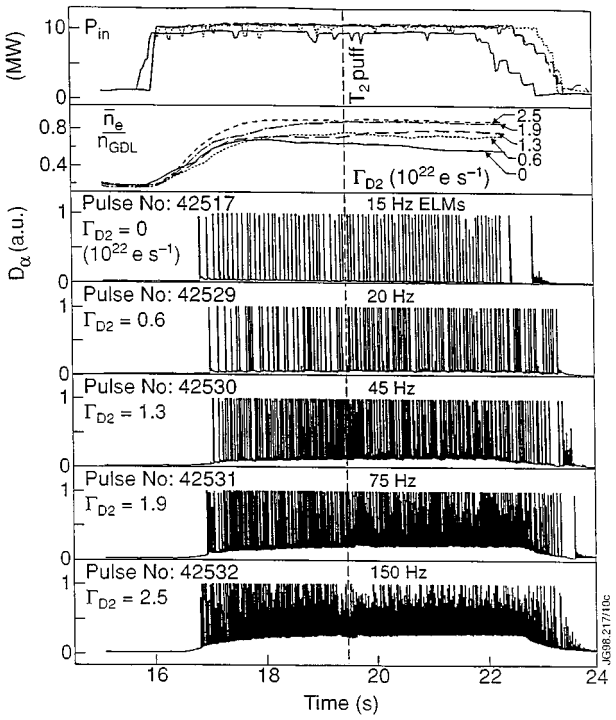

Figure 7. A series of 2 MA/2 T plasmas with different deuterium fuelling rates (Γ_{D2} in electrons per second) into which diagnostic tritium puffs were introduced. The density saturates at ∼90% of the Greenwald value.

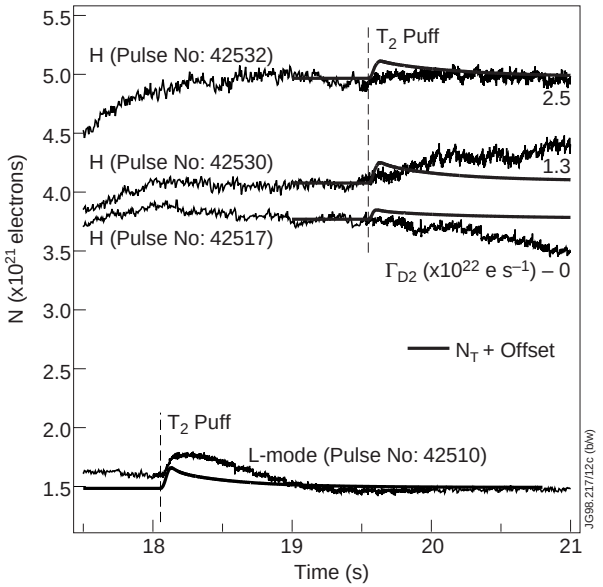

Figure 8. Response of total electron content N in L and H mode plasmas to trace tritium gas puffs. Solid curves show the increase expected from the jump in total triton content N_T as measured by the neutron diagnostics [6].

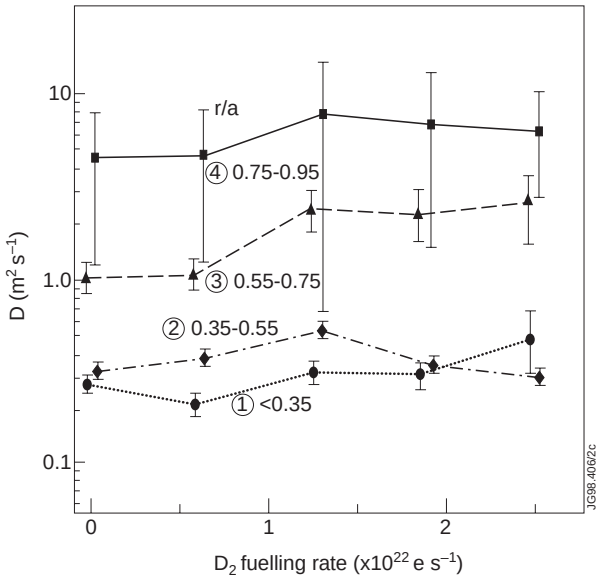

Figure 9. Diffusivity versus fuelling rate for the fuelling scan of Fig. 7. The radial extent of each independent zone for which the particle transport is calculated is indicated [6].

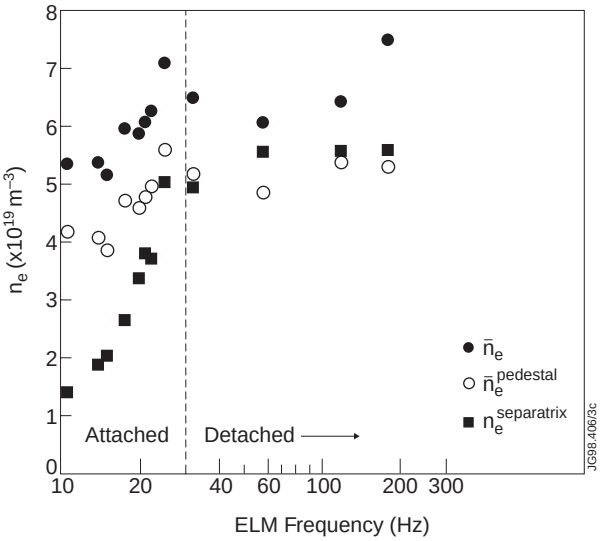

Figure 10. Variation of separatrix density, pedestal density and line averaged density with ELM frequency for a series of 2.5 MA/2.5 T low triangularity discharges in the MkIIa divertor with 12 MW of NBI heating. In attached cases separatrix density is determined by the 'onion skin' method and in detached cases reciprocating probe measurements are used [22]. The pedestal density is a line averaged value measured at 3.75 m; the local density at this radius is about 20% higher in all cases.

4.2. Separatrix density saturation

The separatrix density behaviour in gas fuelled H modes has been determined using 'onion skin' modelling [22] of the SOL in which divertor Langmuir probe measurements are extrapolated upstream [23]. This technique only works for attached plasmas. In detached cases, main chamber reciprocating Langmuir probe measurements have been used where the absolute position with respect to the separatrix has been determined in the attached phase from pressure balance considerations. The results of this analysis are presented in Fig. 10 and show that the ratio of separatrix to line averaged density is strongly dependent on the ELM frequency and hence gas fuelling rate. The low triangularity cases are comparable to the discharges of Fig. 7. At ELM frequencies above those shown, at the point where the separatrix density approaches the pedestal value, the plasma becomes detached.

The results in Fig. 10 show that while the separatrix density is strongly increased by gas fuelling, the pedestal density is not, implying a degradation of the particle transport in the pedestal. Once the separatrix approaches the pedestal value it becomes the major contributor to the overall density. The ultimate density limit therefore seems to be associated with saturation of the separatrix density. This appears to be associated with divertor plasma detachment [21], although a causal link has not yet been established.

5. Discussion and conclusion

High density, high radiated power fraction and small ELMs are key elements of the current ITER design. In JET, gas fuelling and/or impurity seeding reduces the ELM amplitude (Fig. 11). However, it is clear that in JET there is a trade-off between ELM size and τ_E. Since ELMs are often irregular the maximum size may be more important than the average and so both values are shown in Fig. 11. To get the maximum ELM size below the 2% level thought tolerable for ITER implies a significant loss in energy confinement. However, in making this comparison the implicit assumption is made that the pedestal will contribute a similar fraction of the total stored energy in ITER to that in JET. This assumption may not be valid [17].

In JET, the best performance in terms of the normalized Lawson product $f_{GL}H_{97}$ is obtained with unfuelled or lightly fuelled type I ELMy H modes.

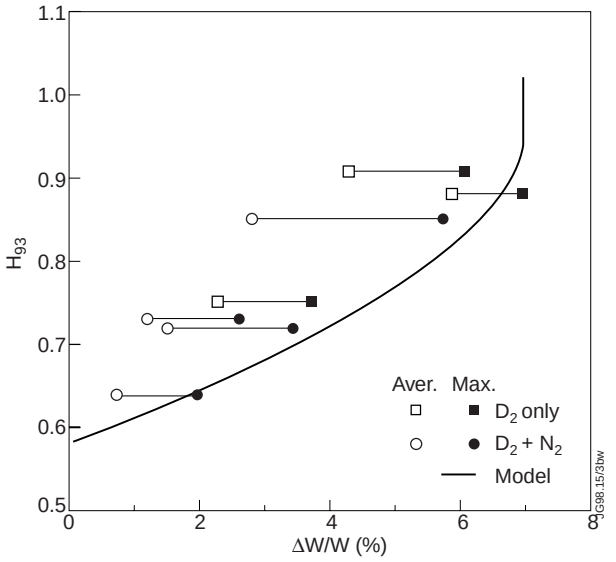

Figure 11. H_{93} versus ELM size ($\Delta W/W$) for a series of D_2 and N_2 seeded discharges with $\delta \approx 0.23$, $I_p = 2.5$ MA, $B_T = 2.5$ T and $P_{NBI} \approx 12$ MW. Average and maximum ELM sizes are compared with the semiempirical model for the ELM pressure cycles [10].

Strong gas fuelling produces a relatively small gain in density and this is at the price of a reduced energy confinement time. Raising the radiated power fraction to achieve type III ELMs and low divertor power loading results in a 25% reduction in confinement time corresponding to a loss in average pedestal pressure. The only effective way found to increase the value $f_{GL}H_{97}$ is by raising the plasma triangularity.

The JET results are consistent with the predictions of a semiempirical model for the ELM pressure cycles relating the ELM frequency to the average pedestal pressure [10]. It is clear from this work that the scaling of the core contributions and that of the edge contributions to the global energy confinement need to be considered independently [17]. However, a limitation of the semiempirical model is that it assumes a knowledge of the ELM frequency; it also assumes that each ELM takes the edge plasma pressure down to a similar base level. Attention has tended to be focused on the scaling of the critical pressure for type I ELMs but this model highlights the fact that the scaling of the lower limit of the pressure cycles is just as important and is currently not understood. It is also evident that the main jump in ELM frequency, and hence the largest loss in averaged pedestal pressure, are associated with the transition from type I to type III ELMs. At present there is no conclusive explanation for this transition. Collisionality at the pedestal or further out near the separatrix may play a role but it is clearly not the only factor. Ideas about the role of fast particles show promise for understanding why type III ELMs are always seen with ICRH and why the neutral beam mass and energy affect the critical pressure for type I ELMs in hot ion H modes. In the next hydrogen campaign planned for JET, comparisons will be made between pulses with deuterium NBI into hydrogen plasmas (D into H) and those with D into D, H into D and H into H. This should show clearly whether it is the bulk ions or fast particles which are determining the pedestal physics.

The JET results on pedestal scaling need to be viewed in the context of results from other machines. Both ASDEX Upgrade [24] and DIII-D [25] have found, like JET, that the critical pressure gradient before a type I ELM scales in a way that is consistent with the ideal ballooning limit. In both machines the pedestal width can be directly determined. The ASDEX Upgrade results suggest that the pedestal width is essentially constant [24], while those from DIII-D [25] are more consistent with the JET results being proportional to the poloidal ion gyroradius.

The loss of pedestal energy associated with strong gas fuelling and high radiated power fraction seen in JET may be acceptable provided that the core confinement scaling is gyro-Bohm-like, as indicated by recent JET results. The lack of strong temperature profile resilience seen in JET would also help ITER owing to the relatively peaked alpha heating profile. However, more work is required on the scaling of radiative regimes and discharges close to the density limit. Dimensionless identity pulses with the ASDEX Upgrade completely detached H mode are currently under investigation. These are expected to show whether the conventional dimensionless parameters ρ^*, ν^*, β and q_{95} are sufficient for identity in the transport [26]. If not, then this would imply that atomic physics is playing a role [27].

Density saturation in H mode appears to have two distinct phases. In the first, gas fuelling raises the separatrix density much more rapidly than it does the pedestal, probably because of enhanced particle transport associated with the increasing ELM frequency. In the second phase, the separatrix density saturates at a value close to that of the pedestal. At this point the divertor plasma becomes increasingly detached. Trace tritium experiments have shown that despite the density saturation the fraction of puffed tritons which reach the core remains high.

This implies that mixture control is still possible even when the gas fuelling efficiency with respect to the total electron density has gone to zero.

References

[1] Greenwald, M., et al., Nucl. Fusion **28** (1988) 2199.
[2] Cordey, J.G., ITER Confinement and Modelling Working Group, Plasma Phys. Control. Fusion **39** (1997) B115.
[3] Janeschitz, G., et al., in Fusion Energy 1996 (Proc. 16th Int. Conf. Montreal, 1996), Vol. 2, IAEA, Vienna (1997) 755.
[4] Horton, L.D., et al., Plasma Phys. Control. Fusion **38** (1996) A269.
[5] Saibene, G., et al., in Controlled Fusion and Plasma Physics (Proc. 24th Eur. Conf. Berchtesgaden, 1997), Vol. 21A, Part I, European Physical Society, Geneva (1997) 49.
[6] Matthews, G.F., et al., J. Nucl. Mater. **266–269** (1999) 1134.
[7] Saibene, G., et al., in Controlled Fusion and Plasma Physics (Proc. 25th Eur. Conf. Prague, 1998), Vol. 22C, European Physical Society, Geneva (1998) Paper B-26.
[8] JET Team, Monk, R.D., Nucl. Fusion **39** (1999) this issue.
[9] JET Team, Plasma Phys. Control. Fusion **37** (1995) A227.
[10] Fishpool, G., Nucl. Fusion **38** (1998) 1373.
[11] Lingertat, J., et al., J. Nucl. Mater. **266–269** (1999) 124.
[12] Saibene, G., et al., Nucl. Fusion **39** (1999) 1133.
[13] JET Team, Parail, V.V., Nucl. Fusion **39** (1999) this issue.
[14] Parail, V.V., Guo, H.Y., Lingertat, J., Nucl. Fusion **39** (1999) 369.
[15] Chankin, A., Saibene, G., Plasma Phys. Control. Fusion (in press).
[16] JET Team, Zastrow, K.-D., Nucl. Fusion **39** (1999) this issue.
[17] JET Team, Cordey, J.G., Nucl. Fusion **39** (1999) this issue.
[18] JET Team, in Fusion Energy 1996 (Proc. 16th Int. Conf. Montreal, 1996), Vol. 1, IAEA, Vienna (1997) 189.
[19] Matthews, G.F., et al., Nucl. Fusion **39** (1999) 19.
[20] Kallenbach, A., et al., Nucl. Fusion **35** (1995) 1231.
[21] Borrass, K., Lingertat, J., Schneider, R., Contrib. Plasma Phys. **38** (1998) 130.
[22] Stangeby, P.C., et al., J. Nucl. Mater. **241–243** (1997) 358.
[23] Davies, S.J., et al., J. Nucl. Mater. **266–269** (1999) 1028.
[24] Suttrop, W.L., et al., Plasma Phys. Control. Fusion **40** (1998) 771.
[25] Groebner, R.J., Osborne, T.H., Phys. Plasmas **5** (1998) 1800.
[26] Connor, J.W., Taylor, J.B., Nucl. Fusion **17** (1977) 1047.
[27] Lackner, K., Comments Plasma Phys. Control. Fusion **15** (1994) 359.

(Manuscript received 3 December 1998
Final manuscript accepted 6 April 1999)

E-mail address of G.F. Matthews: gfm@jet.uk

Subject classification: F1, Te